ACS OMEGA

Open Access

http://pubs.acs.org/journal/acsodf

Article

Efficient Photopolymerization of Dental Resin Composites Using the Photoluminescent Long Afterglow of $Sr_2MgSi_2O_7:Eu^{2+},Dy^{3+}$

Zezhou Hu, Jia Xu, Yongsheng Wang,* Lingdan Xu, Yangman Yi, Bin Liu,* and Zhaofeng Wang*

Cite This: *ACS Omega* 2023, 8, 32396−32403

Read Online

ACCESS | Metrics & More | Article Recommendations

ABSTRACT: Dental curing light with blue emission acts as the excitation source for the photopolymerization of the dental composite resin to achieve dental repairing. However, the current repair methods still suffer from a low monomer conversion degree and incomplete resin curing. In this study, novel dental resin composites (DRCs) were prepared by combining $Sr_2MgSi_2O_7:Eu^{2+},Dy^{3+}$ (SMSED), a photoluminescent material with a blue long afterglow, and dental resin composites. The curing depth, double bond conversion, elastic modulus, compressive strength, water absorption and solubility, and cytotoxicity were investigated systematically. The results suggest that adding 1 wt % SMSED to dental resin composites can maximize the curing depth and double bond conversion rate of DRCs and reduce its water absorption capacity without affecting the mechanical properties and biological toxicity. This work explores the practical applications of SMSED in dental resin composites, which provides an important reference for further improving the effect of dental caries repair.

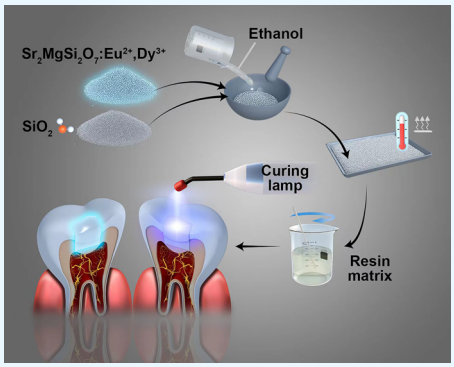

1. INTRODUCTION

Caries is a kind of dental hard tissue damage caused by a variety of factors in the oral cavity, manifested as inorganic demineralization and decomposition of organic matter.[1−3] The continuous development of caries can cause chewing disorders and even tooth loss, which has severe influence on the living quality of patients. As a major common oral disease, caries is listed as one of the three priority diseases for prevention and treatment by the World Health Organization.[4] How to treat caries effectively is recognized as a very important research topic. At present, caries treatment involves first removing the infection in the cavity and then filling the cavity with professional materials to stop the development of the lesion. Subsequently, the appearance and function of the teeth gradually recover to prevent further infection of the pulp. Clinical studies indicate that silver amalgam, glass ionomer cement, and dental resin composites (DRCs) are the most commonly used materials for filling and repairing caries.[5] Compared with the other two materials, DRCs have excellent mechanical properties, good biocompatibility, and aesthetic appearance, and hence, they gradually occupy a major position in the field of dental restoration. DRCs consist of a viscous bisphenol-A glycidyl dimethacrylate (Bis-GMA), a reactive diluent triethyleneglycol dimethacrylate (TEGDMA), and a photoinitiator such as camphorquinone (CQ), which can be photopolymerized using blue light to repair caries.[6,7] The use of bulk-filled composite materials is a recent development in dental technology that aims to simplify the process of filling deep cavities. Unlike the layered filling technology, which requires multiple layers of resin to be applied and cured separately, bulk-filled composites can fill 4−5 mm at once, saving time and reducing the risk of gaps and contamination between layers.[8] However, despite widespread applications, DRCs still suffer from a low monomer conversion degree and incomplete resin curing. The incomplete conversion of the monomer would lead to residual monomers in the resin composites, which could reduce the biocompatibility, durability, and mechanical properties of the dental resin composites.[9] Moreover, the residual monomer would leak into the saliva and stimulate the growth of bacteria around the restoration, resulting in the formation of secondary caries.[10] Likewise, insufficient light curing tends to cause the leaching of uncured components and the formation of gaps between the restoration and the tooth, leading to secondary caries.[11,12] Therefore, improving the curing efficiency and increasing the curing depth (CD) are the main means to enhance the effect of DRC restoration and prevent the occurrence of secondary caries.

The long afterglow photoluminescent materials can absorb and store photon energy in the intrinsic structure and then

Received: March 20, 2023
Accepted: July 24, 2023
Published: August 29, 2023

release the energy in the form of light with a certain wavelength.[13] Under the excitation of an external light source, some excited electrons in the luminescent center of long afterglow materials could be captured and stored by traps with different energy levels.[14] When the external light source is removed, these captured electrons could be released spontaneously to produce continuous luminescence.[15] As a new generation of blue light long afterglow photoluminescent material, $Sr_2MgSi_2O_7$:Eu^{2+},Dy^{3+} (SMSED) has remarkable advantages over other luminescent materials in terms of the chemical and physical stability and afterglow time.[16−18] Meanwhile, it provides the possibility for the application of the material in the field of dental repair. Clinical studies indicate that CQ is the most common photoinitiator system in DRCs, whose light absorption band lies between 400 and 500 nm (λ_{max} = 468 nm).[19] Tertiary amine could be added as a co-initiator to form a photoexcited complex with CQ, instigating and promoting the polymerization via bimolecular interactions.[20] According to the national standard (YY 0055-2018), the operating wavelength of the dental light curing instrument is 365−515 nm, which is used to activate the photoinitiator.[21] Attractively, the required excitation wavelength of SMSED partially coincides with the operating wavelength of the curing light. It suggests that the use of curing light can not only cure DRCs but also stimulate SMSED to produce blue photoluminescence and long afterglow, which can promote the further deep curing of DRCs by CQ.

Based on the above-mentioned considerations, in this work, novel dental resin composites (SMSED/DRCs) were prepared by combining SMSED with DRCs. The curing ability of DRCs was enhanced through the synergistic effect of the curing light irradiation and the blue emissions of SMSED.

2. EXPERIMENTAL SECTION

2.1. Materials. Bisphenol A-glycidyl methacrylate (Bis-GMA, 98%), triethyleneglycol dimethacrylate (TEGDMA, 95%), ethyl-4-dimethylaminobenzoate (4-EDMAB, 99%), and camphorquinone (CQ, 98%) were purchased from Sigma-Aldrich (Shanghai, China). The silane-modified SiO_2 fillers modified from 3-(methacryloxy)propyltrimethoxysilane (γ-MPS, KH570) and particle size ranges from 20 nm were obtained from Yong Wow Wear Resistant Material Co., Ltd. (Hebei, China), and the long afterglow material $Sr_2MgSi_2O_7$:Eu^{2+},Dy^{3+} (SMSED) was purchased from Rui Ying New Material Technology Co., Ltd. (Guangdong, China). All reagents were used directly without purification.

2.2. Preparation of the Dental Restorative Material. The dental restorative material SMSED/DRCs consist of a dental resin matrix and inorganic fillers, including the silane-modified SiO_2 and long afterglow material SMSED. Typically, Bis-GMA and TEGDMA were placed in a magnetic mixer with a ratio of 24.75:24.75 and mixed for 1 h. Then, CQ and 4-EDMAB were added to the above-mentioned hybrid system in the ratio of 0.25:0.25 and mixed for 1 h. The mixed organic matrix accounted for 50% of the total proportion of DRCs. The long afterglow material SMSED (0.5, 1, 2, 4, 6%) and silane-modified SiO_2 fillers were placed in a mortar with anhydrous ethanol to be ground. After drying in an oven at 70 °C for 30 min, the mixture was taken as the inorganic fillers for the resin. The resin matrix and inorganic fillers were mixed in a ratio of 50:50 and stored in a light-proof bottle.

2.3. Curing Depth Measurement. The curing depth (CD) of all samples was determined according to ISO 4049:2019. DRCs were filled into a stainless-steel mold with a diameter of 4 mm and a height of 15 mm and irradiated with curing light from one side for 20 s. Then, the samples were removed from the mold and the uncured part was scraped off with a plastic scraper. The remaining length L (mm, accurate to 0.01) was measured with an electronic vernier caliper, and each group tested five samples separately. The CD value was calculated using eq 1

$$\mathrm{CD} = \frac{L}{2} \tag{1}$$

2.4. Double Bond Conversion (DBC) Measurement. A Fourier transform infrared spectrometer (FTIR) was used to analyze the effect of the SMSED filler on the conversion rate of DRCs. The spectra of the uncured samples were collected first, and then, the spectra of the cured samples were tested after irradiation with curing light for 20 s. The double bond conversion of each SMSED/DRC group was calculated from the ratio of the height of the C═C peak at 1636 cm^{-1} to the height of C═O at 1720 cm^{-1} (H_{1636} and H_{1720} represent the maximum height of the band at 1636 and 1720 cm^{-1}, respectively). Each group tested five samples separately, and the double bond conversion (DBC) was calculated using eq 2

$$\mathrm{DBC}\ (\%) = \left[1 - \frac{(H_{1636}/H_{1720})_{\mathrm{cured}}}{(H_{1636}/H_{1720})_{\mathrm{uncured}}}\right] \times 100\% \tag{2}$$

2.5. Elastic Modulus (EM) and Flexural Strength (FS) Test. The elastic modulus (EM) and flexural strength (FS) were evaluated according to the specifications of ISO 4049:2019. The stainless-steel mold (2 mm × 2 mm × 25 mm) was placed on a polyester film, and then, the samples were filled into the mold and covered with another polyester film, followed by a glass sheet. The samples were irradiated five times for 20 s at a time with partial overlap using wireless curing light. The cured samples were removed from the excess with sandpaper, and the edges were polished and stored away from light at 37 °C for 24 h. A three-point bending test (span 20 mm) was performed using a universal testing machine (AGS-10KN, Shinmazu, Kyoto, Japan) with a crosshead speed of 1.00 mm/min to evaluate EM and FS.

2.6. Compressive Strength (CS) Test. The samples were filled into a stainless-steel mold with a diameter of 4 mm and a height of 6 mm and removed from the mold after 20 s of irradiation with curing light, and five samples were prepared for each group. After curing, the samples were tested on a universal testing machine at a speed of 10 mm/min. The actual diameter d of each resin sample was measured, and the maximum loading force P (N) was recorded until it was damaged. The compressive strength (CS) was calculated using eq 3

$$\mathrm{CS} = \frac{4P}{\pi d^2} \tag{3}$$

2.7. Water Absorption (WS) and Solubility (SL) Tests. The uncured DRCs containing SMSED were added to a disc-shaped poly(tetrafluoroethylene) (PTFE) mold with an inner diameter of 15 mm and height of 1 mm, which was cross-irradiated 8 points from the center to the periphery with each point for 20 s, and then removed from the mold for the next step. The samples were stored in a 37 °C oven, and their weighing was repeated every 24 h until a constant mass was obtained, recorded as m_1. The thickness and diameter of each

https://doi.org/10.1021/acsomega.3c01855
ACS Omega 2023, 8, 32396−32403

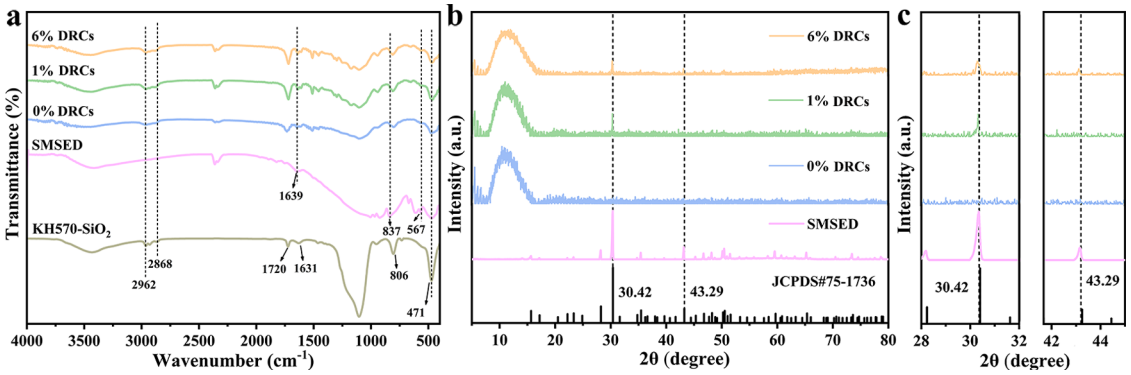

Figure 1. (a) FTIR spectra of the modified SiO_2, SMSED, and DRCs; (b) XRD patterns of SMSED and DRCs with different SMSED contents; and (c) local enlarged XRD patterns.

sample were measured, and the volume (V) was calculated. The samples were individually immersed in 10 mL of distilled water and placed in a 37 °C oven. After 30 days of immersion, the samples were removed, blotted dry with absorbent paper, and weighed immediately, recorded as m_2. Then, the samples were stored in a desiccator, and the weighing was repeated every 24 h until a constant weight was obtained, recorded as m_3. The water absorption (WS) and solubility (SL) values were calculated according to the following eqs 4 and 5, respectively

$$\mathrm{WS}\ (\%) = \frac{(m_2 - m_3)}{V} \times 100\% \tag{4}$$

$$\mathrm{SL}\ (\%) = \frac{(m_1 - m_3)}{V} \times 100\% \tag{5}$$

2.8. Cytotoxicity. *2.8.1. Cell Viability Assay.* Referring to the method GB/T 16886.5-2017, the samples were prepared with 15 mm-diameter, 1 mm-thick circular specimens (surface area of about 400 mm^2) and sterilized overnight under ultraviolet light. A 6-well plate was used, and Dulbecco's modified Eagle medium (DMEM, Gibco) culture solution containing 10% horse serum was added at an immersion ratio of 1.25 cm^2:1 mL according to the surface area of the specimen and culture solution, soaked for 24 h at 37 °C in a 5% CO_2 constant-temperature incubator, and filtered through a 0.2 μm filter to obtain the sample immersion solution. Each 24-well plate was inoculated with 1.5×10^4 logarithmic growth-phase L929 cells, which was cultured in the incubator overnight. After cell adhesion, the control group and the experimental group were set up, and 1 mL of complete medium was added to each well. The cells were continued to be cultured for 1, 2, and 3 days, and cell viability was detected using the CCK-8 Kit.

2.8.2. Live/Dead Cell Assay. Specimens of 15 mm diameter and 1 mm thickness were used for live/dead cell experiments. Each 96-well plate was inoculated with 1×10^4 logarithmic growth-phase L929 cells and placed in the incubator overnight. After sticking to the wall, the control group and the experimental group were set up, and two subwells were set up for each group, and the cells were continued to be cultured for 1 day. Live−dead staining was performed using the LIVE/DEAD cell imaging kit (488/570). The 2× staining solution configured in advance was added and placed at room temperature for 15 min and observed and photographed under a fluorescence microscope.

2.9. Other Characterizations. The chemical structure of DRCs, SMSED, and the modified SiO_2 was characterized by the KBr pellet method using a Thermo Nicolet NEXUS FTIR spectrometer (V70, BRUKER OPTICS, Germany). The phase analysis of DRCs and SMSED was performed using an X-ray diffractometer (XRD-6100, SHIMADZU, Japan). The fluorescence spectra and afterglow decay curves of SMSED were measured using a fluorescence spectrophotometer (Omni-λ300i, ZOLIX, China) equipped with an afterglow tester (PR305, SENSING, China). The surface morphology of DRCs and SMSED was analyzed through a field emission scanning electron microscope (Quanta 650 FEG, FEI, Czech Republic) after Au coating.

3. RESULTS AND DISCUSSION

In order to verify the successful modification of SiO_2 and doping of SMSED into the DRCs, the composite materials and SMSED were characterized by FTIR. The FTIR spectra of the modified SiO_2, SMSED, and DRCs are shown in Figure 1a. For the modified SiO_2, the absorption peaks at 471 and 806 cm^{-1} are attributed to the bending vibration of the Si−O bond and Si−C bond, respectively. The characterization peaks appearing at 2962, 2868, and 1720 cm^{-1} are symmetric and asymmetry stretching vibrations toward $-CH_2$ and the stretching vibration absorption peak of the C=O group, respectively, indicating the presence of organic matter on the surface of SiO_2 and the chemical grafting reaction with the coupling agent, which verifies the successful modification of SiO_2.[22,23] The absorption bands of silicate groups are clearly evident in the observed FTIR spectrum of SMSED. The absorption peak at 567 cm^{-1} belongs to the Si−O−Si bending vibration, which can also be attributed to the presence of the SiO_4 group or Sr−O bending vibration. The peaks at 837 and 1639 cm^{-1} can be attributed to the bending vibrations of Mg−O and Mg^{2+}, respectively. The above-mentioned characteristics confirm the presence of Mg and Sr in SMSED.[24−27] However, these absorption bands almost shift or disappear in the spectra of DRCs, indicating that the SiO_2 and SMSED are involved in the DRCs. In addition, the phase analysis of SMSED and DRCs was conducted by X-ray diffraction measurements, as shown in Figure 1b,c. It is clearly found that all the diffraction peaks of SMSED are consistent with those in the JCPDS file, indicating that SMSED is a pure phase. The diffraction peaks of DRCs show the characteristic peaks of SMSED at 30.42 and 43.29°, which correspond well with those of SMSED. It indicates that

https://doi.org/10.1021/acsomega.3c01855
ACS Omega 2023, 8, 32396−32403

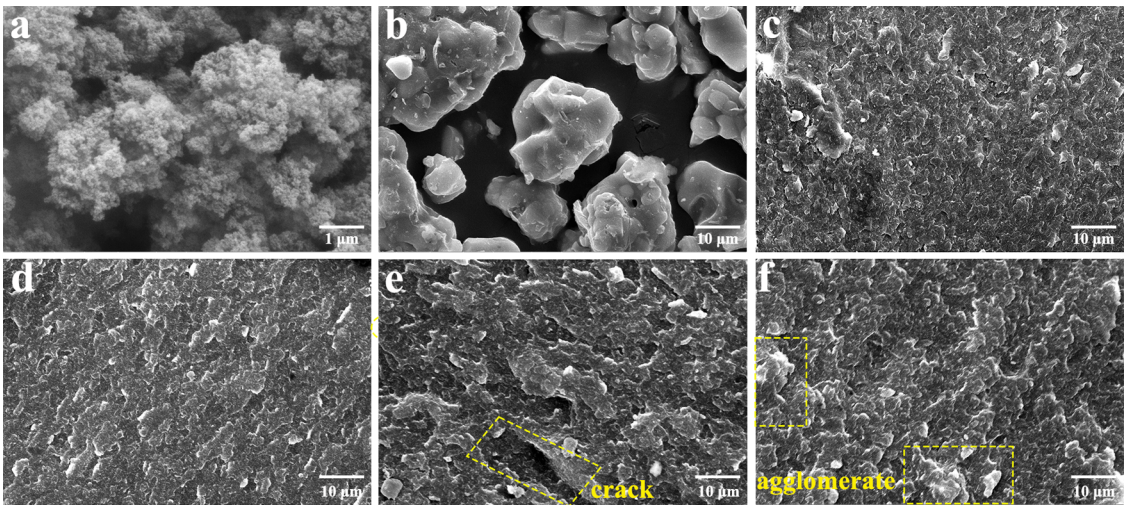

Figure 2. SEM images of (a) modified SiO_2, (b) SMSED, and (c–f) DRCs containing 0, 1, 4, and 6% SMSED.

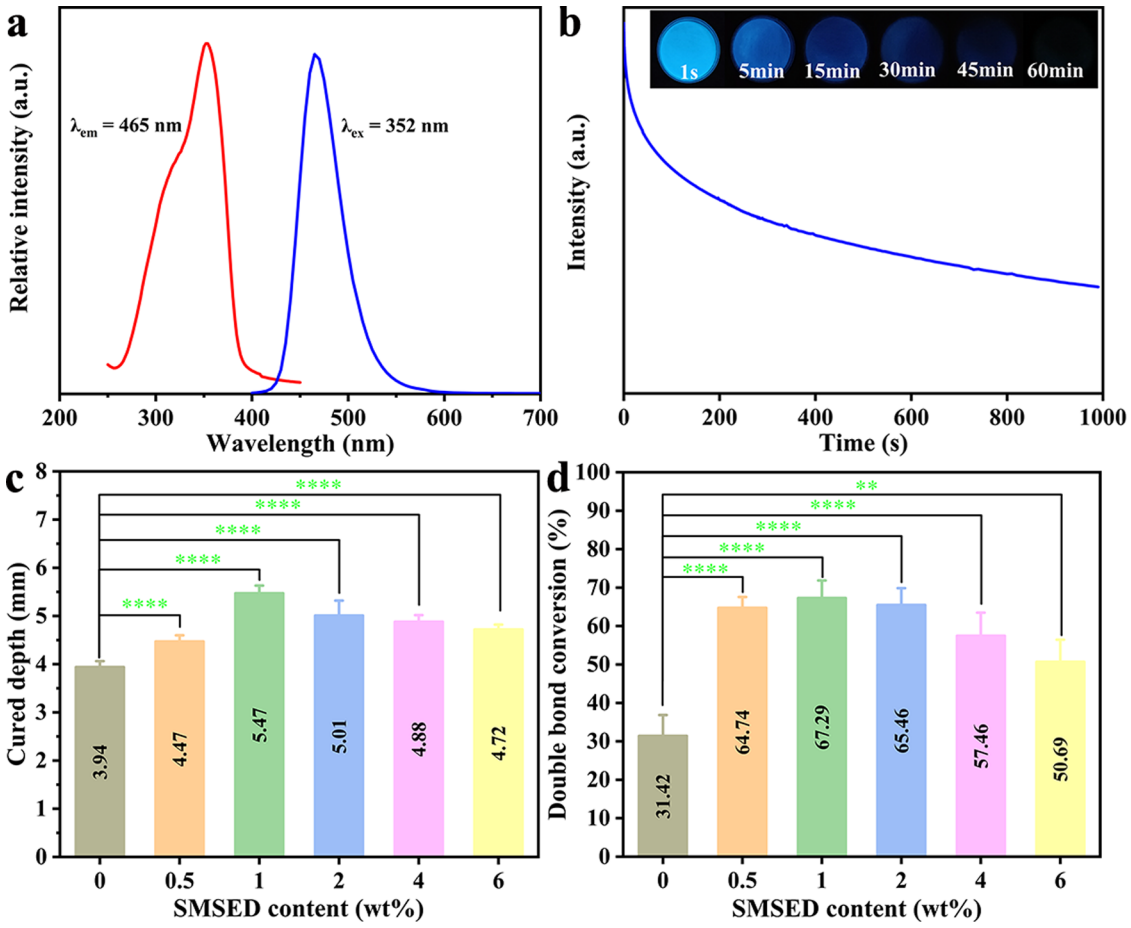

Figure 3. (a) Excitation and emission spectra of SMSED; (b) afterglow decay curve and corresponding optical images of SMSED; and (c) cured depth and (d) double bond conversion of SMSED/DRCs.

SMSED has been successfully doped into DRCs, which is consistent with the result of FTIR.

The SEM images of the modified SiO_2, SMSED, and DRCs are shown in Figure 2. The modified SiO_2 has an obvious agglomeration phenomenon and irregular morphology of particles (Figure 2a), and the SMSED shows irregular and tightly packed particles with good surface morphology (Figure 2b). Fracture surfaces of DRCs containing 0, 1, 4, and 6% SMSED were selected to study their interfacial interactions (Figure 2c–f). Compared with DRCs without SMSED, DRCs containing SMSED have a relatively loose and finer fracture surface. With the increase of the content, the high concentration of SMSED cannot be evenly dispersed in the matrix, and the agglomerates of SMSED will act as areas of stress concentration where cracks are more likely to initiate. In addition, SMSED is completely coated with the matrix without

https://doi.org/10.1021/acsomega.3c01855
ACS Omega 2023, 8, 32396−32403

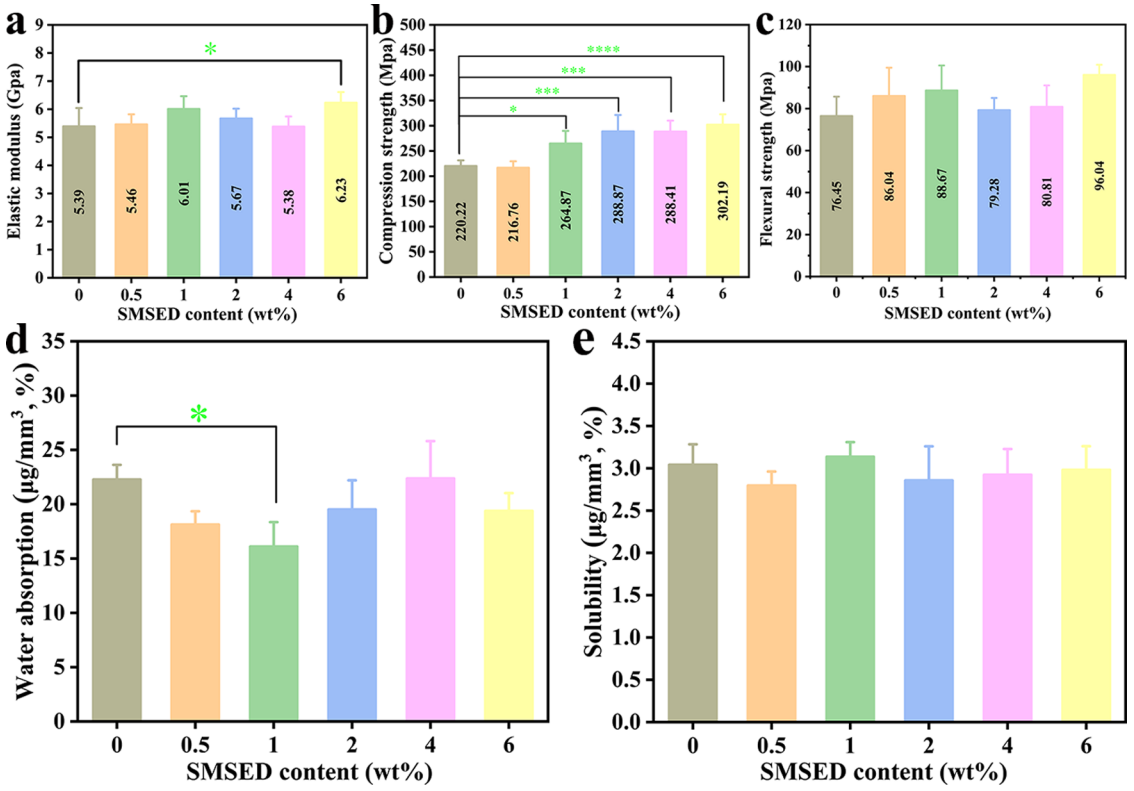

Figure 4. Mechanical properties of DRCs: (a) elastic modulus; (b) compression strength; (c) flexural strength; (d) water absorption; and (e) water solubility.

exposure, indicating that the matrix has interfacial adhesion ability.

The photoluminescence spectra and afterglow decay curve of SMSED are shown in Figure 3. The excitation spectrum is recorded in the range of 250−450 nm, and the emission spectrum is collected in the range of 400−600 nm (Figure 3a). It is observed that both of the spectra are broad. The excitation band monitored at 465 nm should be attributed to the transition of Eu^{2+} from the ($4f^7$) ground state to the excited state $4f^65d^1$ ($4f^7 \rightarrow 4f^65d^1$) configuration. The emission spectrum excited at 352 nm is attributed to the characteristic emission of Eu^{2+} ($4f^65d^1 \rightarrow 4f^7$). The optimal excitation and emission wavelengths of SMSED are 352 nm and 465 nm, respectively, which well match the operating wavelength (365−515 nm) of the dental photocuring instrument. The SMSED also exhibits a prominent afterglow after removing the excitation source. The afterglow decay curve monitored at 465 nm was measured after 10 min of irradiation, and the digital images were taken every 5 min (Figure 3b). The luminescence afterglow first decays rapidly after the light source is removed, followed by prolonged phosphorescence. The afterglow of SMSED shows high brightness and blue color. The above-mentioned phenomenon indicates that the dental light curing instrument can stimulate the photoluminescence of SMSED in the DRCs while repairing caries, and the blue afterglow property of SMSED is further helpful for the deep curing of SMSED/DRCs.

CD depends on the nature of the cure of the resin, such as the contained monomer and the initiator, the nature of the filler, and the thickness of the resin.[28,29] Meanwhile, CD is also influenced by the light source, such as wavelength and curing time.[30] The CD results of DRCs are shown in Figure 3c with the increase of the SMSED content. It is found that the CD of DRCs increases first and then decreases and reaches the maximum depth of 5.47 mm when the content of SMSED is 1%. This may be because SMSED particles can be more dispersed in the matrix, so that it can be more fully excited by the light source to emit light. When the content of SMSED is less than 1%, the CD of DRCs increases with the increase of the SMSED content. The main reason is that the photoluminescence and afterglow properties of SMSED are enhanced, thus improving the CD of DRCs. On the contrary, the excessive SMSED will agglomerate in the matrix and form stress concentration areas, resulting in DRCs being more prone to crack and also unable to achieve the deep curing effect. According to the ISO 4049, the CD of DRCs with a value higher than 2 mm could meet the requirements of clinical applications. The addition of SMSED can significantly improve the CD of DRCs and reduce the workload and cost of dental caries repair. The CD of DRCs is evaluated by FTIR. As shown in Figure 3d, the double bond conversion of all DRCs after light curing is higher than that of the blank group without adding SMSED. When the SMSED content is 1%, the DBC of DRCs reaches the maximum 67.29%. These results are consistent with those of CD, confirming that the addition of SMSED has a significant increase in the curing efficiency of the resin. It is well known that the higher DBC and CD could lead to higher volumetric shrinkage of the DRCs. However, it should be noted that the employed resin composites have been doped by SiO_2 with a weight ratio of 50% and aim toward bulk filling in clinical applications, which could effectively reduce the volume shrinkage of the DRCs.[31,32] Therefore, the effects of the increased DBC and CD by SMSED on the volumetric shrinkage of the resin composite should be very limited.

https://doi.org/10.1021/acsomega.3c01855
ACS Omega 2023, 8, 32396−32403

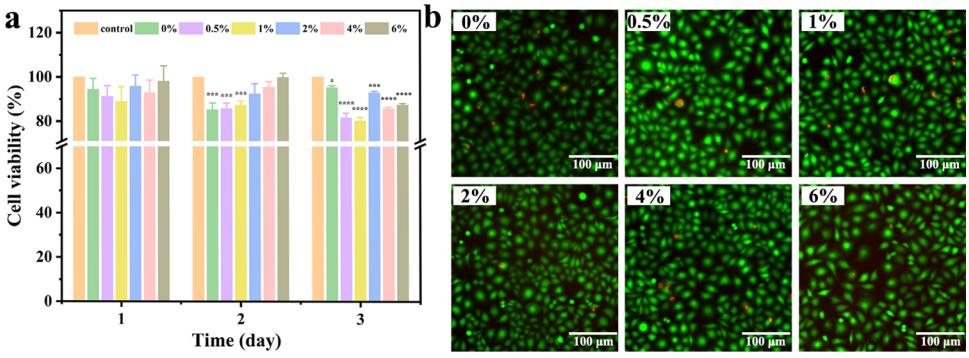

Figure 5. (a) Cytotoxicity test of DRCs and (b) fluorescence images of the live−dead cell.

The dental restorative materials should have sufficient mechanical properties to guarantee their service life. Therefore, it is of great clinical significance to study the mechanical properties of these materials. One of the main reasons for the failure of dental composite prosthesis is the fracture due to insufficient mechanical properties.[6,33] The mechanical properties are affected by the curing efficiency. In addition, the inorganic fillers also play important roles in improving the mechanical properties. As shown in Figure 4, the mechanical properties of DRCs, including the elastic modulus (EM) (Figure 4a), compressive strength (CS) (Figure 4b), and flexural strength (FS) (Figure 4c), were tested using a universal testing machine. The addition of the SMSED filler has almost no effect on the EM and FS of DRCs, while the CS value shows a slight increase with the increase of the SMSED content. Generally speaking, the addition of a micron inorganic filler can improve the mechanical properties of the material to a certain extent. Moreover, the SMSED can improve the mechanical properties of DRCs by increasing the curing depth of the material. However, the different rigidities of the organic matrix and inorganic filler as well as the large packing size can increase the stress concentration at the packer−matrix interface, which makes it more prone to crack. Therefore, the mechanical properties of dental composites are limitedly improved.

The water absorption capacity and solubility are important indexes to evaluate the repair effect of restorative materials. When the aqueous solution comes into contact with the dental material, the water molecules can penetrate and diffuse into the polymer chains of the material, causing the material to slightly expand or deform, leading to its separation from the tooth or even fall out.[34,35] The solubility of dental restorative materials can cause dimensional instability, crack formation, and loosening of the material under internal stress and eventually lead to the fracture of the restorative material.[36] Therefore, the water absorption capacity (Figure 4d) and solubility (Figure 4e) of DRCs are evaluated. Compared with the blank group without SMSED, the DRCs containing 1% SMSED show significantly lower water absorption, which should relate to its relatively dense surface. Moreover, the solubility of DRCs containing SMSED exhibits no significant change compared with the blank group without SMSED. It indicates that DRCs containing 1% SMSED have good structural and dimensional stability, meeting the ISO 4049 standard.

Biocompatibility is an important indicator for the biomedical materials, and the cell viability assay is commonly used to assess cytotoxicity. The extracts of DRCs were incubated with L929 fibroblasts for 1, 2, and 3 days, and the test results are shown in Figure 5a. The results suggest that DRCs with different SMSED contents have no obvious toxicity to cells at the incubation time of 1, 2, and 3 days. In addition, the survival rate of the corresponding cells is more than 70%, which is considered safe for DRCs. Therefore, it is promising for the future application in oral cavity. The fluorescence images of the live−dead cells are shown in Figure 5b, where green and red represent living and dead cells, respectively. The experimental results indicate that the presence of DRCs has no significant effect on the death of L929 cells, which provides feasibility for clinical use.

4. CONCLUSIONS

In summary, this work provides a systematic analysis of a novel dental composite to provide high curing efficiency without compromising other properties of the resin. The incorporation of 1% SMSED into dental composites shows the best curing properties with little influence on mechanical properties. Compared with the control group without SMSED, the water absorption of DRCs is significantly decreased, and the solubility is not significantly changed. Furthermore, the cytotoxicity of the dental DRCs shows good results on cell viability. The presence of SMSED in DRCs shows negligible cytotoxicity against the L929 cell line.

AUTHOR INFORMATION

Corresponding Authors

Yongsheng Wang − *State Key Laboratory of Solid Lubrication, Lanzhou Institute of Chemical Physics, Chinese Academy of Sciences, Lanzhou, Gansu 730000, China*; Email: wysh0304@licp.cas.cn

Bin Liu − *School/Hospital of Stomatology, Lanzhou University, Lanzhou, Gansu 730000, China*; Email: liubkq@lzu.edu.cn

Zhaofeng Wang − *State Key Laboratory of Solid Lubrication, Lanzhou Institute of Chemical Physics, Chinese Academy of Sciences, Lanzhou, Gansu 730000, China; Shandong Laboratory of Yantai Advanced Materials and Green Manufacturing, Yantai, Shandong 265503, China*; orcid.org/0000-0003-3641-7011; Phone: +86-931-4968682; Email: zhfwang@licp.cas.cn

Authors

Zezhou Hu − *School/Hospital of Stomatology, Lanzhou University, Lanzhou, Gansu 730000, China; State Key Laboratory of Solid Lubrication, Lanzhou Institute of Chemical Physics, Chinese Academy of Sciences, Lanzhou, Gansu 730000, China*

https://doi.org/10.1021/acsomega.3c01855
ACS Omega 2023, 8, 32396−32403

Jia Xu − *School/Hospital of Stomatology, Lanzhou University, Lanzhou, Gansu 730000, China; State Key Laboratory of Solid Lubrication, Lanzhou Institute of Chemical Physics, Chinese Academy of Sciences, Lanzhou, Gansu 730000, China*

Lingdan Xu − *School/Hospital of Stomatology, Lanzhou University, Lanzhou, Gansu 730000, China*

Yangman Yi − *School/Hospital of Stomatology, Lanzhou University, Lanzhou, Gansu 730000, China*

Complete contact information is available at: https://pubs.acs.org/10.1021/acsomega.3c01855

Notes

The authors declare no competing financial interest.

■ ACKNOWLEDGMENTS

This work was supported by the National Natural Science Foundation of China (81970976) and the Natural Science Foundation for Distinguished Young Scholars of Gansu Province (20JR5RA572).

■ REFERENCES

(1) Li, H.; Hou, B. X. Strengthening the prevention and treatment of caries in patients receiving systemic therapy. *Chin. J. Stomatol.* **2021**, *56*, 10−15.

(2) Machiulskiene, V.; Campus, G.; Carvalho, J. C.; Dige, I.; Ekstrand, K. R.; Jablonski-Momeni, A.; Maltz, M.; Manton, D. J.; Martignon, S.; Martinez-Mier, E. A.; Pitts, N. B.; Schulte, A. G.; Splieth, C. H.; Tenuta, L. M. A.; Zandona, A. F.; Nyvad, B. Terminology of dental caries and dental caries management: consensus report of a workshop organized by ORCA and cariology research group of IADR. *Caries Res.* **2020**, *54*, 7−14.

(3) Huang, Q. T.; Liang, Z. L.; Li, J. D.; Bai, Y.; He, J. W.; Lin, Z. M. Size dependence of particulate calcium phosphate fillers in dental resin composites. *ACS Omega* **2021**, *6*, 35057−35066.

(4) Wen, P. Y. F.; Chen, M. X.; Zhong, Y. J.; Dong, Q. Q.; Wong, H. M. Global burden and inequality of dental caries, 1990 to 2019. *J. Dent. Res.* **2022**, *101*, 392−399.

(5) Cho, K.; Rajan, G.; Farrar, P.; Prentice, L.; Prusty, B. G. Dental resin composites: a review on materials to product realizations. *Composites, Part B* **2022**, *230*, No. 109495.

(6) Yadav, R.; Lee, H.; Lee, J.-H.; Singh, R. K.; Lee, H.-H. A comprehensive review: physical, mechanical, and tribological characterization of dental resin composite materials. *Tribol. Int.* **2023**, *179*, No. 108102.

(7) Yang, J. X.; Liao, M. Y.; Hong, G. Y.; Dai, S. Q.; Shen, J. D.; Xie, H. F.; Chen, C. Effect of APTES- or MPTS-conditioned nanozirconia fillers on mechanical properties of Bis-GMA-based resin composites. *ACS Omega* **2020**, *5*, 32540−32550.

(8) Wang, K.; Li, B.; Ni, K.; Li, B.; Wang, Z. Optimal photoinitiator concentration for light-cured dental resins. *Polym. Test.* **2021**, *94*, No. 107039.

(9) Oréfice, R.; Discacciati, J. A. C.; Neves, A. D.; Mansur, H. S.; Jansen, W. C. In situ evaluation of the polymerization kinetics and corresponding evolution of the mechanical properties of dental composites. *Polym. Test.* **2003**, *22*, 77−81.

(10) Askar, H.; Krois, J.; Gostemeyer, G.; Bottenberg, P.; Zero, D.; Banerjee, A.; Schwendicke, F. Secondary caries: what is it, and how it can be controlled, detected, and managed? *Clin. Oral Invest.* **2020**, *24*, 1869−1876.

(11) Askar, H.; Krois, J.; Gostemeyer, G.; Schwendicke, F. Secondary caries risk of different adhesive strategies and restorative materials in permanent teeth: Systematic review and network meta-analysis. *J. Dent.* **2021**, *104*, No. 103541.

(12) Nedeljkovic, I.; De Munck, J.; Vanloy, A.; Declerck, D.; Lambrechts, P.; Peumans, M.; Teughels, W.; Van Meerbeek, B.; Van Landuyt, K. L. Secondary caries: prevalence, characteristics, and approach. *Clin. Oral Invest.* **2020**, *24*, 683−691.

(13) Zhan, T. Z.; Xu, C. N.; Yamada, H.; Terasawa, Y.; Zhang, L.; Iwase, H.; Kawai, M. Enhancement of afterglow in $SrAl_2O_4$:Eu^{2+} long-lasting phosphor with swift heavy ion irradiation. *RSC Adv.* **2012**, *2*, 328−332.

(14) Liu, B.; Shi, C.; Yin, M.; Dong, L.; Xiao, Z. The trap states in the $Sr_2MgSi_2O_7$ and $(Sr,Ca)MgSi_2O_7$ long afterglow phosphor activated by Eu^{2+} and Dy^{3+}. *J. Alloys Compd.* **2005**, *387*, 65−69.

(15) Yang, E.; Hai, O.; Ren, Q.; Wu, X.; Pei, M.; Xu, D.; Zhu, J. Improved trap capability of shallow traps of $Sr_2MgSi_2O_7$:Eu^{2+},Dy^{3+} through depositing Au nanoparticles. *J. Alloys Compd.* **2021**, *858*, No. 157705.

(16) Liang, W.; Zhang, W.; Xu, X.; Zhang, S.; Yao, X.; Chen, J. Versatile up-converted emission microcrystals assisted photocuring for dental restorations. *Opt. Mater.* **2022**, *128*, No. 112371.

(17) Stepuk, A.; Mohn, D.; Grass, R. N.; Zehnder, M.; Krämer, K. W.; Pellé, F.; Ferrier, A.; Stark, W. J. Use of NIR light and upconversion phosphors in light-curable polymers. *Dent. Mater.* **2012**, *28*, 304−311.

(18) Fernández-Rodríguez, L.; Balda, R.; Fernández, J.; Durán, A.; Pascual, M. J. Role of Eu^{2+} and Dy^{3+} concentration in the persistent luminescence of $Sr_2MgSi_2O_7$ glass-ceramics. *Materials* **2022**, *15*, 3068.

(19) Santini, A.; Gallegos, I. T.; Felix, C. M. Photoinitiators in dentistry: a review. *Prim. Dent. J.* **2013**, *2*, 30−33.

(20) Hamidi, A. S.; Hadis, M. A.; Palin, W. M. Alternative co-initiators for photocurable dental resins: polymerisation, quantum yield of conversion and cytotoxicity. *Dent. Mater.* **2022**, *38*, 1330−1343.

(21) Price, R. B. T. Light curing in dentistry. *Dent. Clin. North Am.* **2017**, *61*, 751−778.

(22) Zhou, Y. S.; Yu, J. R.; Wang, X. X.; Wang, Y.; Zhu, J.; Hu, Z. M. Preparation of KH570-SiO_2 and their modification on the MF/PVA composite membrane. *Fibers Polym.* **2015**, *16*, 1772−1780.

(23) Liu, Y.; Lin, Q.; Chen, J.; Shao, Y.; Wang, Y.; Wang, J. PDMS-OH and nano-SiO_2 modified KH570-TEOS silica-sol coating and protective effect on concrete. *Colloids Surf., A* **2022**, *648*, No. 129279.

(24) Jyothi, K. R.; Bhagya, K. R.; Nagabhushana, H.; Hegde, V. N.; Murugendrappa, M. V.; Prakash, A. P. G.; Prasad B, D.; Nagabhushana, N. M. Synthesis and characterization of advanced functional dysprosium doped $Sr_2MgSi_2O_7$ nanopowders for white LED application. *Phys. B* **2020**, *590*, No. 412195.

(25) Tshabalala, M. A.; Swart, H. C.; Dejene, F. B.; Coetsee, E.; Ntwaeaborwa, O. M. Structure, surface analysis, photoluminescent properties and decay characteristics of Tb^{3+}-Eu^{3+} co-activated $Sr_2MgSi_2O_7$ phosphor. *Appl. Surf. Sci.* **2016**, *360*, 409−418.

(26) Sahu, I. P.; Bisen, D. P.; Brahme, N.; Wanjari, L.; Tamrakar, R. Luminescence properties of $Sr_2MgSi_2O_7$:Eu^{2+},Ce^{3+} phosphor by solid state reaction method. *Phys. Procedia* **2015**, *76*, 80−85.

(27) Shrivastava, R.; Kaur, J. Characterisation and mechanoluminescence studies of $Sr_2MgSi_2O_7$: Eu^{2+}, Dy^{3+}. *J. Radiat. Res. Appl. Sci.* **2015**, *8*, 201−207.

(28) Hasanain, F. A. Flexural strength and depth of cure of single shade dental composites. *J. Pharm. Res. Int.* **2021**, *33*, 110−118.

(29) Romano, B. D.; Soto-Montero, J.; Rueggeberg, F. A.; Giannini, M. Effects of extending duration of exposure to curing light and different measurement methods on depth-of-cure analyses of conventional and bulk-fill composites. *Eur. J. Oral Sci.* **2020**, *128*, 336−344.

(30) Hasslen, J. A.; Barkmeier, W. W.; Shaddy, R. S.; Little, J. R. Depth of cure of high-viscosity bulk-fill and conventional resin composites using varying irradiance exposures with a light-emitting diode curing unit. *J. Oral Sci.* **2019**, *61*, 425−430.

(31) Gonçalves, F.; Azevedo, C. L.; Ferracane, J. L.; Braga, R. R. Bis-GMA/TEGDMA ratio and filler content effects on shrinkage stress. *Dent. Mater.* **2011**, *27*, 520−526.

(32) Gonçalves, F.; Campos, L. M. P.; Rodrigues-Júnior, E. C.; Costa, F. V.; Marques, P. A.; Francci, C. E.; Braga, R. R.; Boaro, L. C.

C. A comparative study of bulk-fill composites: degree of conversion, post-gel shrinkage and cytotoxicity. *Braz. Oral Res.* **2018**, *32*, No. e17.
(33) Zhang, X. Y.; Zhang, Q.; Meng, X.; Ye, Y. T.; Feng, D. S.; Xue, J.; Wang, H. B.; Huang, H. F.; Wang, M.; Wang, J. Rheological and mechanical properties of resin-based materials applied in dental restorations. *Polymers* **2021**, *13*, 2975.
(34) Hassan, S. A.; Beleidy, M.; EI-din, Y. A. Biocompatibility and surface roughness of different sustainable dental composite blocks: comprehensive in vitro study. *ACS Omega* **2022**, *7*, 34258−34267.
(35) Moslehifard, E.; Ghaffari, T.; Abolghasemi, H.; Maleki Dizaj, S. Comparison of conventional pressure-packed and injection molding processing methods for an acrylic resin denture based on microhardness, surface roughness, and water sorption. *Int. J. Dent.* **2022**, *2022*, 11−16.
(36) Alzraikat, H.; Burrow, M. F.; Maghaireh, G. A.; Taha, N. A. Nanofilled resin composite properties and clinical performance: a review. *Oper. Dent.* **2018**, *43*, E173−E190.

https://doi.org/10.1021/acsomega.3c01855
ACS Omega 2023, 8, 32396−32403